MINERVA CHIR 2009;64:521-39

Clinically-relevent orthotopic metastatic models of pancreatic cancer imageable with fluorescent genetic reporters

M. BOUVET [1], R. M. HOFFMAN [1, 2]

[1]*Department of Surgery*
University of California San Diego
Moores Cancer Center, La Jolla, CA, USA.
[2]*AntiCancer Inc., San Diego, CA, USA*

This article describes authors' cumulative experience with the development and preclinical application of clinically-relevant, metastatic orthotopic mouse models of pancreatic cancer made imageable with genetic reporters. These models utilize the human pancreatic cancer cell lines which have been genetically engineered to selectively express high levels of green fluorescent protein (GFP) or red fluorescent protein (RFP). Tumors with fluorescent genetic reporters are established subcutaneously in nude mice, and fragments of the subcutaneous tumors are then surgically transplanted onto the pancreas. Locoregional tumor growth and distant metastasis of these orthotopic implants occurs spontaneously and rapidly throughout the abdomen in a manner consistent with clinical human disease. Highly specific, high-resolution, real-time quantitative fluorescence imaging of tumor growth and metastasis may be achieved *in vivo* without the need for contrast agents, invasive techniques, or expensive imaging equipment. A high correlation between florescence optical imaging, magnetic resonance imaging, and ultrasound in these models has been demonstrated. Transplantation of RFP-expressing tumor fragments onto the pancreas of GFP- or cyan fluorescent protein-expressing transgenic mice was used to facilitate visualization of tumor-host interaction between the pancreatic cancer cells and host-derived stroma and vasculature. Such *in vivo* models have enabled visualization in real time and acquisition of images of the progression of pancreatic cancer in the live animal, the models also demonstrate the real-time antitumor and antimetastatic effects of several novel therapeutic strategies on pancreatic malignancy. These fluorescent models are therefore powerful and reliable tools with which to investigate metastatic human pancreatic cancer and novel therapeutic strategies directed against it.

Key words: **Green fluorescent proteins - Red fluorescent protein - Cyan fluorescent protein - Pancreas - Pancreatic neoplasm - Mice, nude.**

Pancreatic cancer is often a fatal disease with five-year survival rates of only 1-4%.[1, 2] It is the fourth leading cause of cancer related mortality in the United States. Reasons for low survival in this disease include aggressive tumor biology, high metastatic potential, and late presentation at

Acknowledgments.—This work was supported in part by grants from the National Cancer Institute CA109949 and CA132971 and American Cancer Society RSG-05-037-01-CCE (to M.B.) and National Cancer Institute grant CA103563 (to AntiCancer, Inc.).

Corresponding author: M. Bouvet, Department of Surgery, University of California San Diego, Moores Cancer Center, 3855 Health Sciences Drive 10987, La Jolla, CA 92093-0987, USA. E-mail: mbouvet@ucsd.edu

the time of diagnosis.[3, 4] The symptoms of pancreatic cancer may include jaundice, pain, weight loss, digestive problems, and new onset diabetes.[5] By the time an individual with pancreatic cancer develops these symptoms, the tumor has often reached a large size and metastasized to other organs including liver, lung, and peritoneum.[4] Although chemotherapy can offer some palliation, it is not curative and the median survival is less than six months. For the few patients who have localized disease, surgical resection offers the only chance for cure. However, even with potentially curative surgery the five-year survival rates are only 15-20%.[1] Clearly, techniques for earlier more-effective diagnosis and new treatment modalities need to be explored if progress is to be made. In an effort to help develop more effective treatment modalities for pancreatic cancer and improve detection, we and others have developed orthotopic models of human pancreatic cancer in the nude mouse that simulate tumor growth, progression, and metastasis and allow for testing of novel treatment strategies.[6-15]

Mouse models based on athymic mice have been used for human cancer for the past several decades. However, metastatic rates from subcutaneous or intramuscular xenografts have been low or non-existent, even from tumors that were highly metastatic in the patient from whom the tissues were derived.[16, 17] Work from a number of laboratories indicates that implanting human tumor cells orthotopically in the corresponding organ of nude mice results in much higher metastatic rates.[18-20] For instance, dissociated human colon cancer cells, when grown in culture and subsequently injected into the cecum of nude mice, produce tumors that eventually metastasize to the liver, showing that orthotopic implantation can enhance the metastatic capability of human tumor cells in nude mice.[21] Similar results have been achieved for orthotopic implantation of cell lines of human lung cancer, bladder cancer, melanoma, breast cancer, stomach, colon, and head and neck cancer.[22]

In the 1980s, investigators first reported metastatic models of human pancreatic cancer using orthotopic implantation of tumor-cell suspensions, which resulted in invasive tumor growth and subsequent metastases.[8, 23] Our laboratory first developed the concept of surgical orthotopic implantation (SOI) of tumor fragments which was found to greatly increase the metastatic potential of the implanted tumor.[24] Vezeridis *et al.* used pancreatic tumor tissue for orthotopic transplantation, resulting in extensive local growth, and metastases to liver, lung, and lymph nodes.[10] In 1992, we used histologically intact patient specimens of pancreatic cancer for orthotopic transplantation to nude mice to construct a metastatic model of human pancreatic cancer.[11] This model resembled the clinical picture of pancreatic cancer including: 1) extensive local tumor growth; 2) extension of the locally growing human pancreatic cancer to the nude mouse stomach and duodenum; 3) metastases of the human pancreatic tumor to the nude-mouse liver and regional lymph nodes; and 4) distant metastases of the human pancreatic tumor to the nude-mouse adrenal gland, diaphragm, and mediastinal lymph nodes.[11]

In 1993, we described use of this patient-like model of human pancreatic cancer for the *in-vitro* and *in-vivo* evaluation of the antitumor activity of 5-fluoroocuracil (5-FU) and mitomycin-C (MMC).[13] The antitumor activity of these agents was initially determined in an in-vitro histoculture drug-response assay and inhibition rates were 5.6% for 5-FU and 39.4% for MMC. When the antitumor activities of 5-FU against PANC-4 was determined in vivo using the nude mouse SOI treatment model, slight local tumor growth inhibition with equivalent incidence of metastases to the liver and the peritoneum as the control were observed in the mice treated with 5-FU. In contrast, mice treated with MMC had considerably reduced local tumor growth without liver and peritoneal metastases. Thus the histoculture drug response assay in combination with the SOI metastatic model provided for the first time a paradigm for evaluation of agents that may be effective against not only locally growing human pancreatic cancer but resulting metastases as well.

A number of approaches have been taken to label tumor cells to visualize and track them *in vivo*. Previous attempts to genetically label tumor cells for tracking purposes used the *Escherichia coli* β-galactosidase (*lacZ*) gene to detect micrometastases.[25] However, detection of *lacZ* requires extensive histological preparation, with sacrifice of the tissue and/or animal: therefore, it was not possible to image, visualize, and study tumor cells in real-time in viable fresh tissue or in the live animal.

The ability to confer real-time visualization and imaging of tumor growth and progression in viable fresh tissue and in the live animal would be an important factor in the development of a real-time reporter gene for metastasis and recurrence. Several approaches have been developed with this goal in mind: Fukumura *et al.* and Chambers *et al.* labeled tumor tissue with fluorescent dyes. However, these methods are not suitable for long-term metastasis studies.[26, 27] Weissleder *et al.* have infused tumor-bearing animals with protease-activated near-infrared fluorescent probes.[28] Tumors with appropriate proteases could activate the probes and could be imaged externally. The limits to such a system include much higher liver to tumor background precluding liver metastasis imaging, which is among the most important metastatic sites; the stated time limit of 96 hours, which precludes growth and efficacy studies; the requirement of appropriate tumor protease activity; and the requirement of selective tumor delivery of the probes.

Another attempt involved insertion of the luciferase gene into tumor cells such that they emit light.[29] However, luciferase enzymes transferred to mammalian cells require the exogenous injected delivery of their luciferin substrate, an invasive and impractical requirement in an intact animal. The resolution of this approach is low, due to low signal strength, requiring anesthesia since long periods are needed for photon counting. With this technology, there is insufficient photon flux to form a true image. Also, it is not known whether luciferase genes can function stably over significant time periods in tumors and in the metastases derived from them.

It became clear that higher signal strength, specificity, resolution, and physiological conditions were necessary to report the natural course of tumor progression and metastasis on a real-time basis. The green fluorescent protein (GFP) gene, cloned from the bioluminescent jellyfish *Aequorea victoria*, was chosen to satisfy these conditions because it has demonstrated its great potential for use as a cellular marker.[30-32] GFP cDNA encodes a 283-aa monomeric polypeptide with a molecular mass of 27 kDa that requires no other *Aequorea* proteins, substrates, or cofactor to fluoresce.[33, 34] GFP gene gain-of-function bright mutants have been generated by various techniques that have been humanized for high expression.[35-38]

A major advantage of GFP-expressing tumor cells is that imaging requires no preparative procedures, contrast agents, substrates, anesthesia, or light-tight boxes as do other imaging techniques.[39] As pioneered by our laboratory, GFP imaging is thus uniquely suited for whole-body imaging of tumor growth and metastases in live animals.[40-42] We have developed technology that has enabled the stable transduction of the GFP gene into a large series of human tumor cell lines.[43-54] The tumor cell lines were able to stably express GFP at high levels both *in vitro* and *in vivo*. We have previously demonstrated the important parameter that GFP-expressing cancer cells could be directly visualized in fresh tissues of transplanted animals at a very high resolution down to the sub-cellular level.[43-47] With this technology, we were able to visualize tumor cells that had seeded with or without subsequent colonization in all the major organs, including liver, lung, brain, spinal cord, axial skeleton, and lymph nodes.[43-47] We have developed orthotopic GFP metastatic models of lung cancer,[48] prostate cancer,[49] melanoma,[50] colon cancer,[51] and other cancers as well.[55] These results demonstrated that GFP gene-transfected tumor cells represent a new tool to study tumor cell growth, dissemination, invasion, metastasis, and progression through all stages.

GFP models of pancreatic cancer

We developed *in vivo* models of GFP-expressing pancreatic cancer in the nude mouse.[6, 7] To understand the metastatic pattern of pancreatic cancer, we developed stable high-expression GFP transductants of human pancreatic cancer cell lines. Fragments of subcutaneous-growing GFP-expressing tumors were implanted by surgical orthotopic implantation (SOI) in the pancreas of nude mice or by portal vein injection of a cell suspension. Subsequent micrometastases were visualized by GFP fluorescence in the peritoneum, periportal lymph nodes, liver, and lung as well as other sites in the abdominal cavity. The use of GFP-expressing MiaPaCa-2 and BxPC-3 cells transplanted by SOI or by portal vein injection revealed the extensive metastatic potential of pancreatic cancer. Furthermore, the primary tumor and subsequent metastasis were visualized by whole body imaging through the skin of the nude mouse without the need for laparotomy.[7] Such visualization can be a practical and convenient way to follow metastasis in a "real-time" fashion. We have also described a novel, highly metastatic model of pancreatic cancer that utilizes pancreatic cancer cells engineered to express very high levels of *Discosoma sp.* red fluorescent protein (RFP).[56-62] These RFP-expressing pancreatic tumors can be implanted into the pancreas of transgenic GFP nude mice to create dual color models to study tumor host interactions.[63, 64] These new metastatic models are plasing a critical role in the study of the mechanism of metastasis in pancreatic cancer and in screening of therapeutics that prevent or reverse this process. These models are described in detail below.

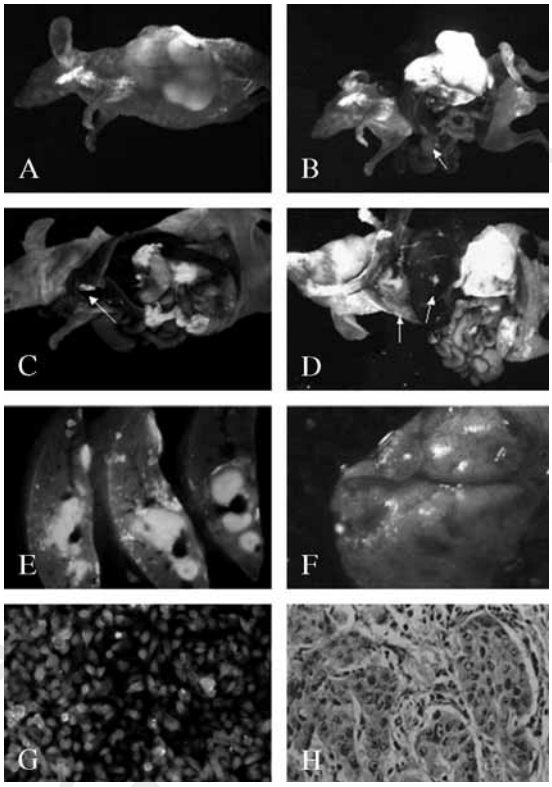

Figure 1.—A) The BxPC-3-GFP pancreatic tumor transplanted by surgical orthotopic implantation (SOI) is externally visualized with fluorescence through the skin of the nude mouse; B) laparotomy of the same mouse in (A) showing locally advanced BxPC-3-GFP tumor with portal lymph node metastases; C) the primary tumor formed in the pancreas at 12 weeks after SOI is visualized under bright-field microscopy. Numerous metastases and micrometastases can be visualized by GFP under fluorescence microscopy in the stomach, spleen, periportal nodes (arrow), liver, and mediastinum (arrow); D) MIA PaCa-2-GFP tumor at week-10 post-SOI. Left arrow shows diaphragm metastases and right arrow shows liver metastases; E) multiple high expressing GFP liver metastases are noted under fluorescence microscopy; F) GFP-expressing lung metastases are noted; G) the human pancreatic cancer cell line MIA PaCa-2 was transduced with the RetroXpress vector pLEIN that expresses enhanced GFP and the neomycin resistance gene on the same bicistronic message. The stable high expression clone was selected in 800 mg/mL of G418; H) H&E section of the MIA PaCa-2-GFP tumor.[6]

Visualization of micrometastasis of pancreatic cancer

In the orthotopic models of pancreatic cancer described above, micrometastases were visualized by GFP fluorescence in the peritoneum, periportal lymph nodes, liver, and lung as well as other sites in the abdominal cavity (Figure 1). The use of GFP-expressing MiaPaCa-2 and BxPC-3 cells transplanted by SOI or by portal vein injection revealed the extensive metastatic potential of pancreatic cancer at the cellular level in vivo. Furthermore, the primary tumor and subsequent metastasis

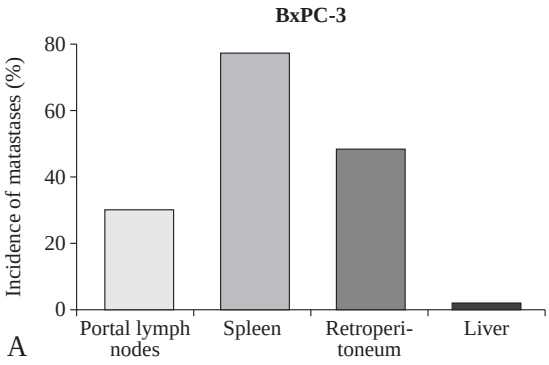

Figure 2.—Site-specific metastases in orthotopic models of human pancreatic cancer. A) BxPC-3-GFP; B) MIA-PaCa-2-GFP. Forty-four and 26 mice were used for the BxPC-3-GFP and MIA-PaCa-2 models, respectively. The y-axis represents cumulative percentage of mice with metastasis.[6]

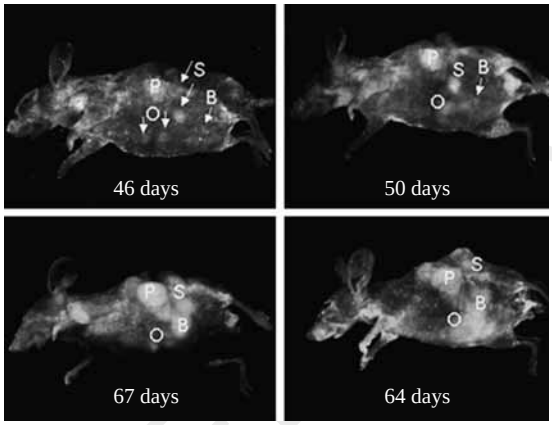

Figure 3.—Consecutive external whole-body images of internally-growing BxPC-3-GFP tumors. A series of external fluorescence images of the BxPC-3-GFP pancreatic tumor in a single animal was obtained from day-46 to day-64 after SOI of BxPC-3-GFP in a nude mouse. On right: growth curves for primary pancreatic tumor (P), splenic metastasis (S), omental metastases (0), and bowel metastasis (B) as determined by whole-body imaging.[7]

were visualized by whole body imaging through the skin of the nude mouse.[7]

Tumor selective metastatic organ targeting by pancreatic cancer

Figure 2 represents the incidence of metastasis in each model at week-20 post-SOI.[6] The BxPC-3-GFP cell line produced locally-advanced, invasive tumors that metastasized regionally and selectively to the spleen and the retroperitoneum with distant liver metastases very rare (Figure 2A). In contrast, metastases in the MIA-PaCa-2 model were selective to distant sites in the portal lymph nodes and liver with regional retroperitoneal lymph node metastasis very rare (Figure 2B).

Real-time whole-body imaging of BxPC-3-GFP primary tumor and multiple metastatic growth

Consecutive whole-body simultaneous images of the primary BxPC-3-GFP pancreatic tumor, spleen, bowel, and omentum metastases are shown in Figure 3A. These images were simultaneously obtained in a single animal on day-46, day-50, day-57, and day-64 after SOI. In each of the sites, tumor growth and progression were quantified with image analysis. Growth curves (Figure 3B) for the primary tumor and metastases at each of the above sites were constructed from the whole-body images. Thus, simultaneous metastases development can be quantified with whole-body imaging.[7]

Sequential intravital images of omental and liver micrometastasis of BxPC-3-GFP

A series of internal intravital fluorescence images of an omental micrometastasis from a BxPC-3-GFP pancreatic tumor in a single animal was obtained from day-36 to day-70 after SOI of BxPC-3-GFP in a nude mouse.[7] The images were acquired during a laparotomy procedure. As determined by intravital imaging, the size of the metastatic lesion grew progressively with time (Figure 4). Figure 5 shows a series of intravital fluorescence images of liver micrometastases following SOI of BxPC-3-GFP in nude mice.

RFP models of pancreatic cancer

We described a novel, highly metastatic model of pancreatic cancer that utilizes pancreatic cancer cells engineered to express very high levels of *Discosoma sp.* red fluorescent protein (RFP).[56-62] This model clinically resembles human pancreatic cancer in

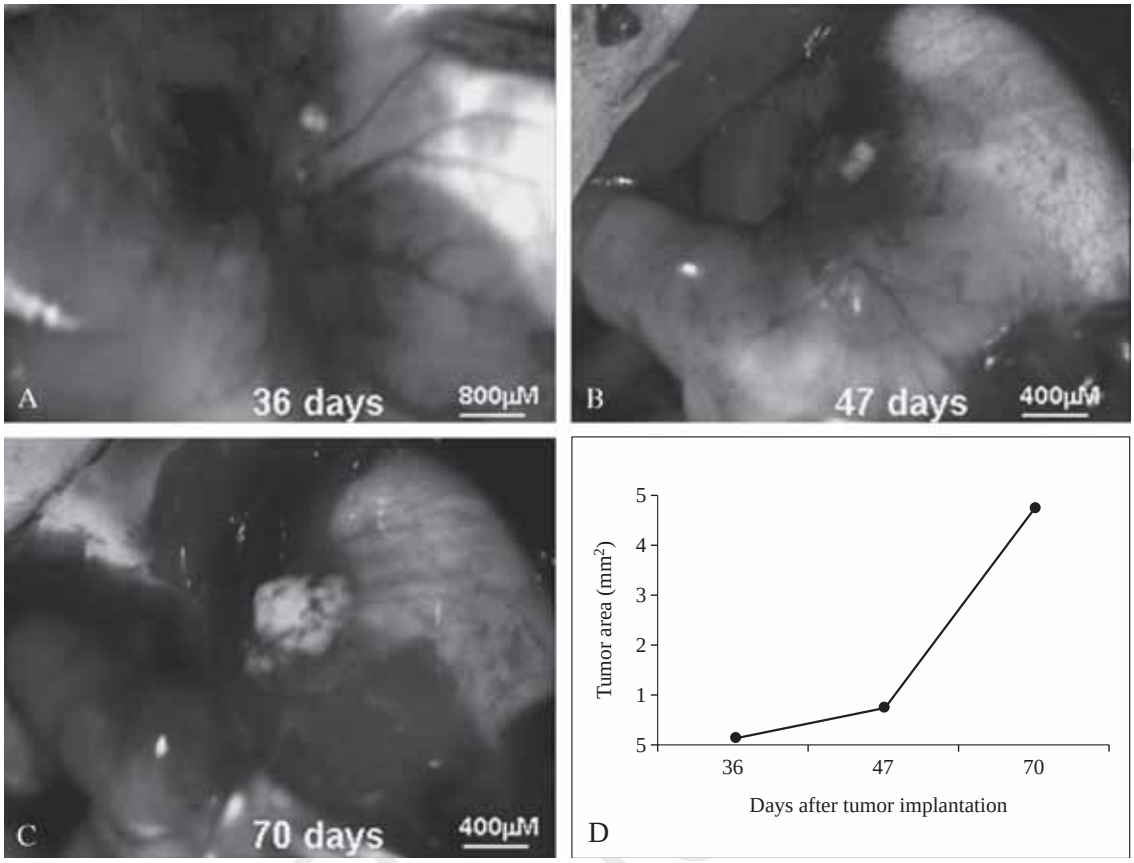

Figure 4.—Sequential intravital images of omental micrometastasis of BxPC-3-GFP. A-C) A series of internal fluorescence images of an omental micrometastasis from a BxPC-3-GFP pancreatic tumor in a single animal was obtained from day-36 to day-70 after SOI of BxPC-3-GFP in a nude mouse during a laparotomy procedure; D) as determined by internal imaging, the size of the metastatic lesion grew progressively with time.[7]

its pattern of growth and metastasis. It rapidly and reliably produces distant metastatic disease, and frequently gives rise to malignant abdominal ascites and peritoneal carcinomatosis. Moreover, the enhanced fluorescence of this model enables real-time visualization and imaging of pancreatic tumor growth and metastasis in the live animal, and permits identification of both macro- and micrometastases (Figure 6). These features make the model an ideal system with which to study the effects of novel antineoplastic agents on tumor growth and metastasis.

Sensitivity of fluorescence imaging

Previously published data describe in detail the reproducibility and sensitivity of our non-invasive fluorescence imaging systems demonstrating that single cells can be imaged depending on the site. Using fairly simple equipment including a CCD camera and light box, we have reproducibly and non-invasively quantitated tumor growth and response to therapy.[6, 7, 43, 51, 54-58, 61, 62, 63-68] With regard to the sensitivity of fluorescence imaging, we have demonstrated that when human pancreatic cancer was surgically orthotopically implanted into nude mice, whole-body optical images visualized, in real time, growth of the primary tumor and its metastatic lesions in the liver and other organs.[6, 7, 49] The depth to which metastasis [51] and micrometastases could be imaged depends on their size and brightness. It should be noted that this sensitivity was achieved with a simple light box

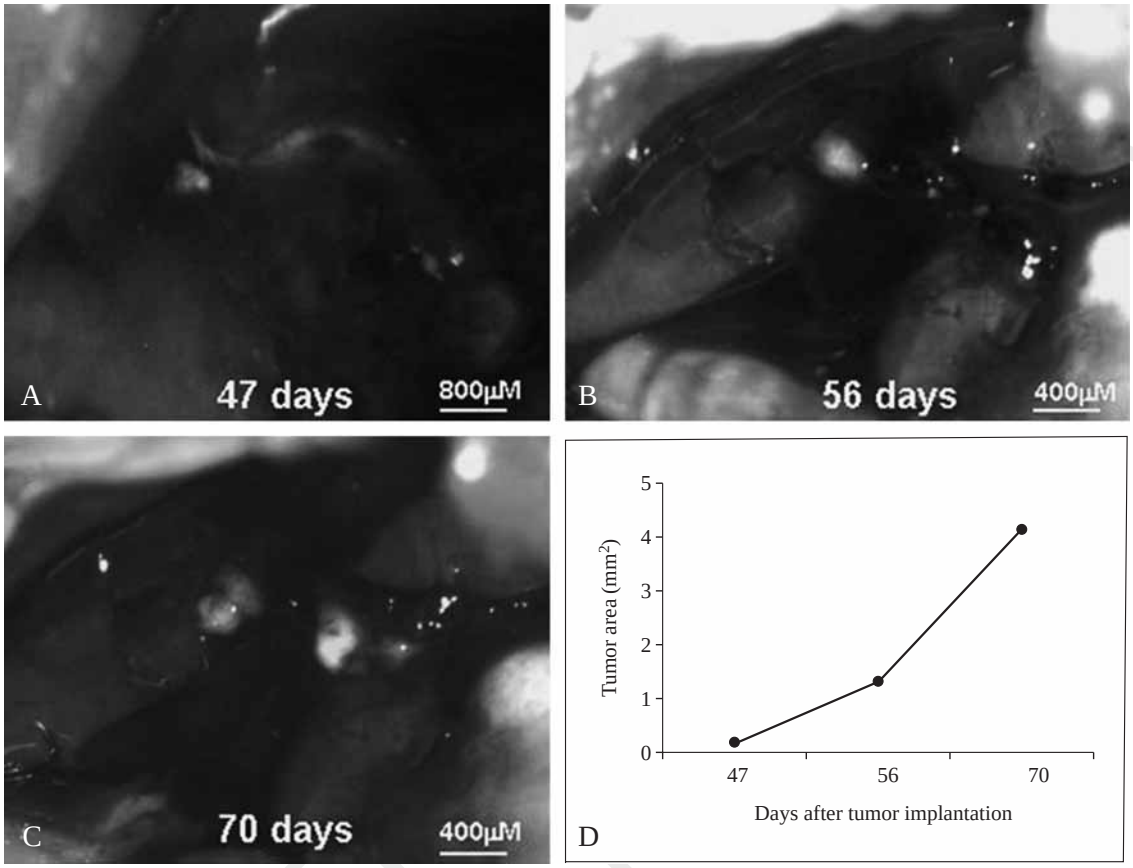

Figure 5.—Sequential intravital images of liver micrometastasis of BxPC-3-GFP. A-C) Internal images of liver metastases following SOI of BxPC-3-GFP tumor in nude mice were obtained during a laparotomy procedure. As determined by internal imaging, the area of the metastatic lesions increased over time.[7]

equipped with a 50-watt mercury lamp. Laser light sources, including multiphoton, now available to us enable greater sensitivity and resolution even deeper in the animal.[69, 70] Our previous studies [60] compared RFP-based imaging of pancreatic tumors to magnetic resonance imaging (MRI) (Figure 7). The fluorescent tumor size can be quantified using image quantification software as we have previously described [58, 62] and appears to be at least as sensitive as MRI.

In another study, we performed whole-body fluorescence imaging and ultrasound imaging to evaluate and to compare these noninvasive imaging modalities for assessing tumor burden and tumor progression in an orthotopic mouse model of pancreatic cancer.[71] The human pancreatic cancer cell line XPA-1, engineered for stable, high-level expression of RFP, was orthotopically implanted into the pancreas of nude mice. The tumors were allowed to grow over a period of one to several weeks during which time the mice were imaged using both fluorescence imaging and ultrasound imaging to measure tumor burden and to monitor tumor growth. Whole-body fluorescence imaging and ultrasound imaging both allowed for the visualization and measurement of orthotopic pancreatic tumor implants *in vivo* (Figure 8). The imaging sessions were well-tolerated by the mice and yielded data which correlated well in the quantitative assessment of tumor burden. Whole-body fluorescence and two-dimensional ultrasound imaging showed a strong correlation for measurement of tumor

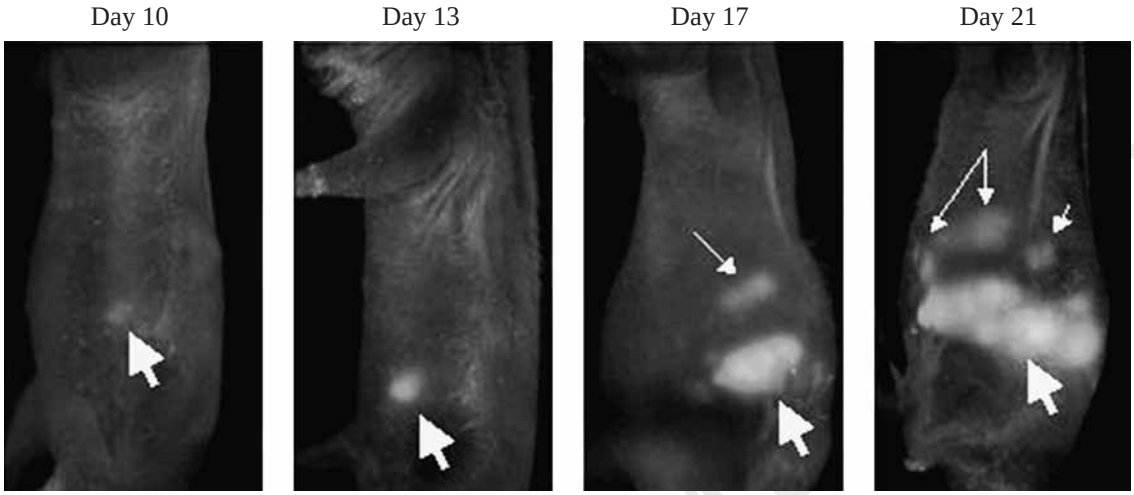

Figure 6.—RFP tumor fluorescence enabled real-time, whole-body imaging of tumor growth and metastasis of MIA-PaCa-2-RFP tumors after surgical orthotopic implantation. Panels represent sequential fluorescent imaging of a single mouse taken on days 10, 13, 17 and 21 after SOI. Progressive primary tumor growth and the development of metastases are clearly visualized through the skin in the live animal. Heavy arrow: primary tumor; thin arrows: metastatic tumor.[7]

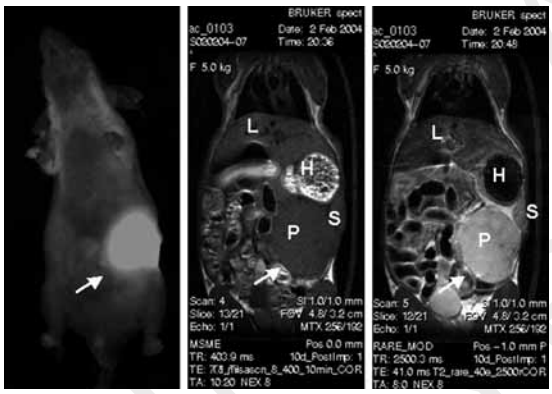

Figure 7.—Visualization of early and locally advanced pancreatic malignancy in an orthotopic nude mouse model by fluorescence optical imaging (FOI) and T1- and T2-weighted MRI. Panels represent a single mouse that underwent serial imaging on day 10 after surgical orthotopic implantation of fluorescent MIA-PaCa-2-RFP human pancreatic cancer fragments. Primary tumor was clearly visible using each imaging strategy. P: pancreas; L: liver; H: stomach; S: spleen.[60]

size over a range of tumor sizes (R(2)=0.6627, P=0.003 for an exposure time of 67 msec and R(2)=0.6553, P=0.003 for an exposure time of 120 ms). Our findings suggest a complementary role for fluorescence imaging and ultrasound imaging in assessing tumor burden and tumor progression in orthotopic mouse models of human cancer.

To confirm a correlation between tumor burden, as determined by non-invasive externally visualized RFP fluorescence, and standard measurements of tumor volume, the primary tumor of each mouse was used.[56, 58, 61] Primary tumor volume was calculated using the formula (long diameter x short diameter^2)/2, where long diameter and short diameter measurements were precisely obtained in the open animal. The externally-visualized RFP fluorescent area of the primary tumor was determined as previously described by placing the mouse in a fluorescent light box equipped with a fiberoptic light source of 470 nm. At each imaging time point, real-time determination of tumor burden was performed by quantifying fluorescent area of the primary tumor.[7, 56] The correlation coefficient (r=0.89) between tumor volume and RFP fluorescence area was highly significant (P<0.05) (Figure 9).

We can increase the sensitivity of imaging down to the single cell level by the use of a simple skin flap in the mouse.[54] Strong fluorescence labeling with green and red fluorescent protein along with inexpensive video detectors, positioned externally to the mouse, allows the monitoring through the skin flap of details of tumor growth, angiogenesis, and metastatic spread. Opening a reversible skin-flap in the light path markedly reduces signal

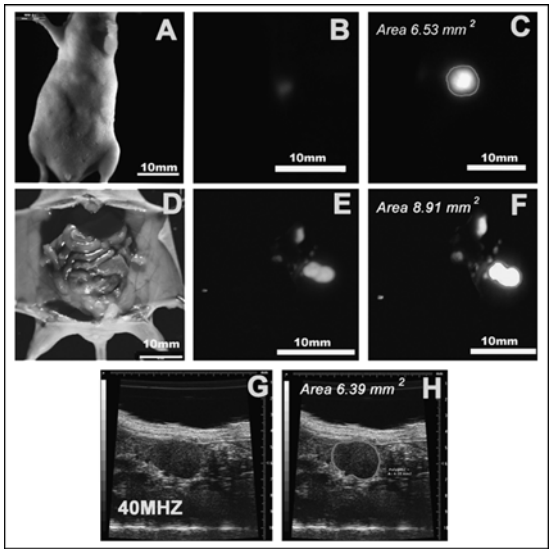

Figure 8.—Comparison of whole body fluorescence imaging and ultrasound imaging to monitor tumor growth over time in individual mice. Whole-body fluorescence and ultrasound images were obtained on a weekly basis for a period of four weeks. Tumor measurements were determined as explained in the legend for Figure 2. A) The graph shows the growth of an orthotopic pancreatic-tumor implant in a single mouse (M1) as assessed by both whole-body fluorescence (FL) and ultrasound (US) imaging. The four corresponding ultrasound (upper row) and fluorescence (lower row) images are shown below the graph with the calculated tumor sizes (mm2) for each image indicated; B) graphical depictions of tumor growth over a four week period for an additional four mice (M2 thru M5) with orthotopic pancreatic tumor implants. Bar graphs shown in this figure depict single measurements taken at weekly timepoints. The graphs demonstrate a strong correlation between whole-body fluorescence and ultrasound imaging modalities for determination of tumor size.[71]

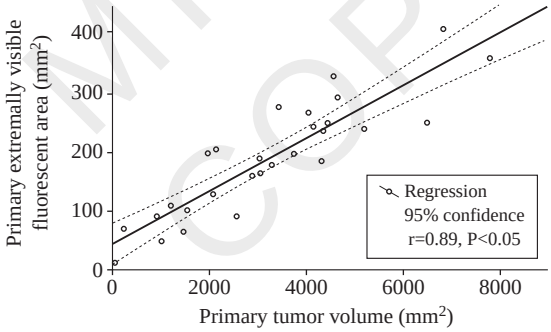

Figure 9.—Red fluorescent area quantified using external fluorescence imaging correlated strongly with tumor volume measured directly. At autopsy, measurement of externally visualized fluorescent area and direct measurements of the primary tumor of each mouse were obtained. A significant correlation (r=0.89, P<0.05) was observed between these values.[56]

attenuation, increasing detection sensitivity many-fold. The observable depth of tissue is thereby greatly increased and many cancer cells that were previously hidden are now clearly observable. We have shown that single tumor cells, expressing GFP, were seeded on the brain and imaged through a scalp skin-flap. Lung tumor micro foci representing a few cells were viewed through a skin-flap over the chest wall, while contralateral micrometastases were imaged through the corresponding skin-flap. Pancreatic tumors and their angiogenic microvessels were imaged by means of a peritoneal wall skin-flap.[54]

Use of RFP models for drug discovery and evaluation

The MIA-PaCa-2 human pancreatic cancer cell line was transduced with RFP and grown subcutaneously. Fluorescent tumor fragments were then surgically transplanted onto the nude mouse pancreas. Groups treated with intraperitoneal gemcitabine or intravenous irinotecan were sequentially imaged to compare, in real time, the antimetastatic and antitumor effects of these agents compared with untreated controls (Figure 10).[56]

We demonstrated the ability of a novel, orally-administered cytosine analog, CS-682, to effectively prolong survival and inhibit metastatic growth in the RFP orthotopic mouse model of pancreatic cancer.[61] We have also used these RFP-expressing models to study adjuvant treatment with CS-682.[62] Seven days after implantation, mice were randomized into eight groups, depending on whether they were to be treated by tumor resection, five weeks of CS-682 chemotherapy at 40-60 mg/kg qd or both. Throughout the course of treatment, non-invasive optical whole-body imaging based on brilliant RFP expression of the tumor permitted visualization and quantification of primary, metastatic, and recurrent disease (Figure 11). Total tumor burden negatively correlated with survival. Untreated mice died of disseminated disease with a median survival of 26 days. Surgical resection alone conferred a small but significant survival

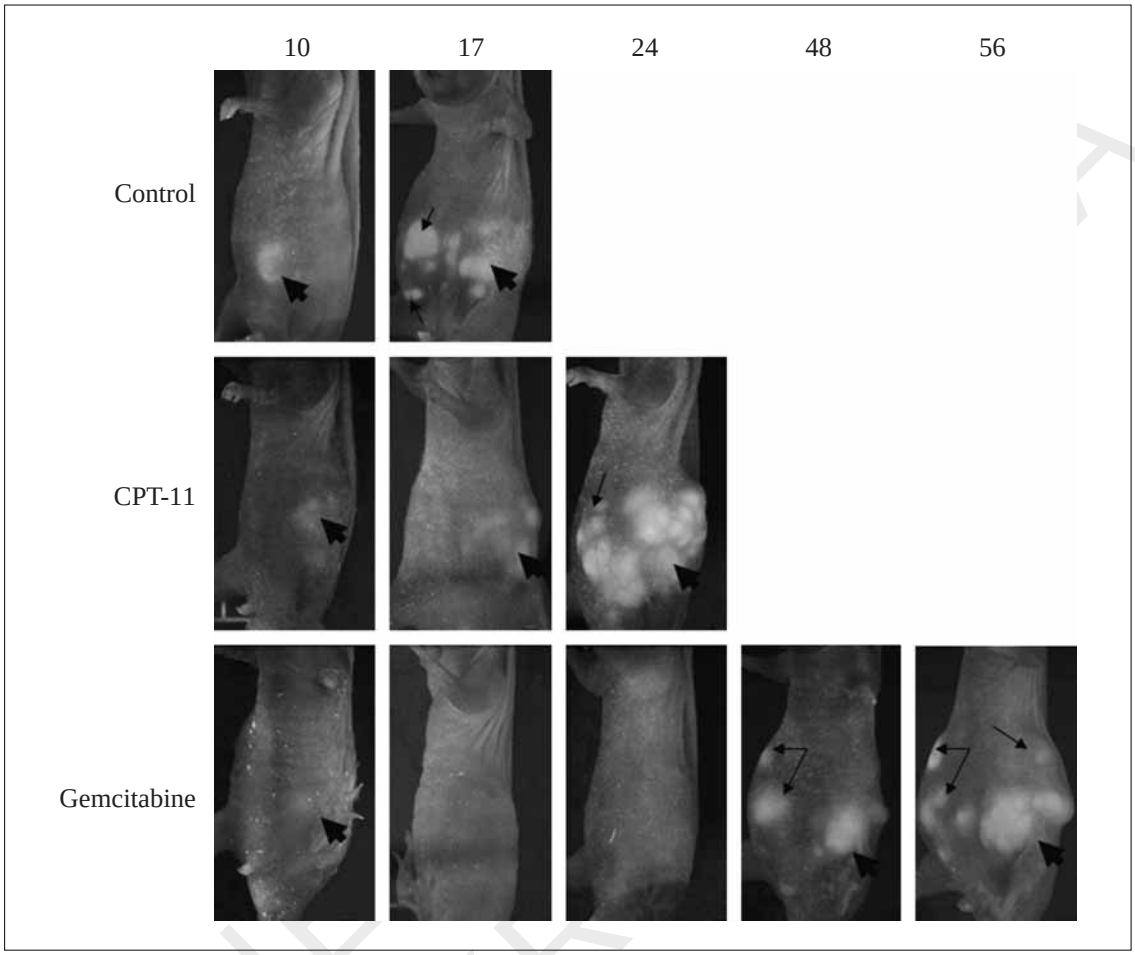

Figure 10.—Real-time, in vivo imaging of MIA-PaCa-2-RFP pancreatic cancer progression and evaluation of therapeutic efficacy over time. Representative mice from each treatment group on days 10, 17, 24, 48, and 56 after tumor implantation are shown. Thick arrows show primary tumor, and thin arrows indicate metastatic tumor. CPT-11 suppressed primary and metastatic tumor growth compared with controls. In contrast, gemcitabine successfully induced temporary regression of disease over the first month, after which growth and distant metastasis of tumor accelerated despite continued treatment.[56]

advantage (median survival 28 days, P=0.03). Primary CS-682 treatment at all doses also significantly prolonged survival compared to untreated animals (P<0.05), and was more effective than surgery alone at doses of 50 mg/kg and 60 mg/kg (median survival 34 days, P=0.045 and 38.5 days P=0.03, respectively). Maximal survival (median 48 days, with 30% of animals surviving longer than 60 days) was achieved by adjuvant CS-682, 50 mg/kg, given after surgical resection of the primary pancreatic tumor (P=0.004 compared to surgery alone). The results demonstrate that adjuvant oral administration of CS-682 for pancreatic cancer is highly effective with acceptable toxicity suggesting its potential for cure of this disease in appropriate combinations.

Bacterial treatment of pancreatic cancer

The RFP-expressing model has also been used to evaluate a tumor-targeting strategy for pancreatic cancer using a modified auxotrophic strain of *Salmonella typhimurium*.[72]

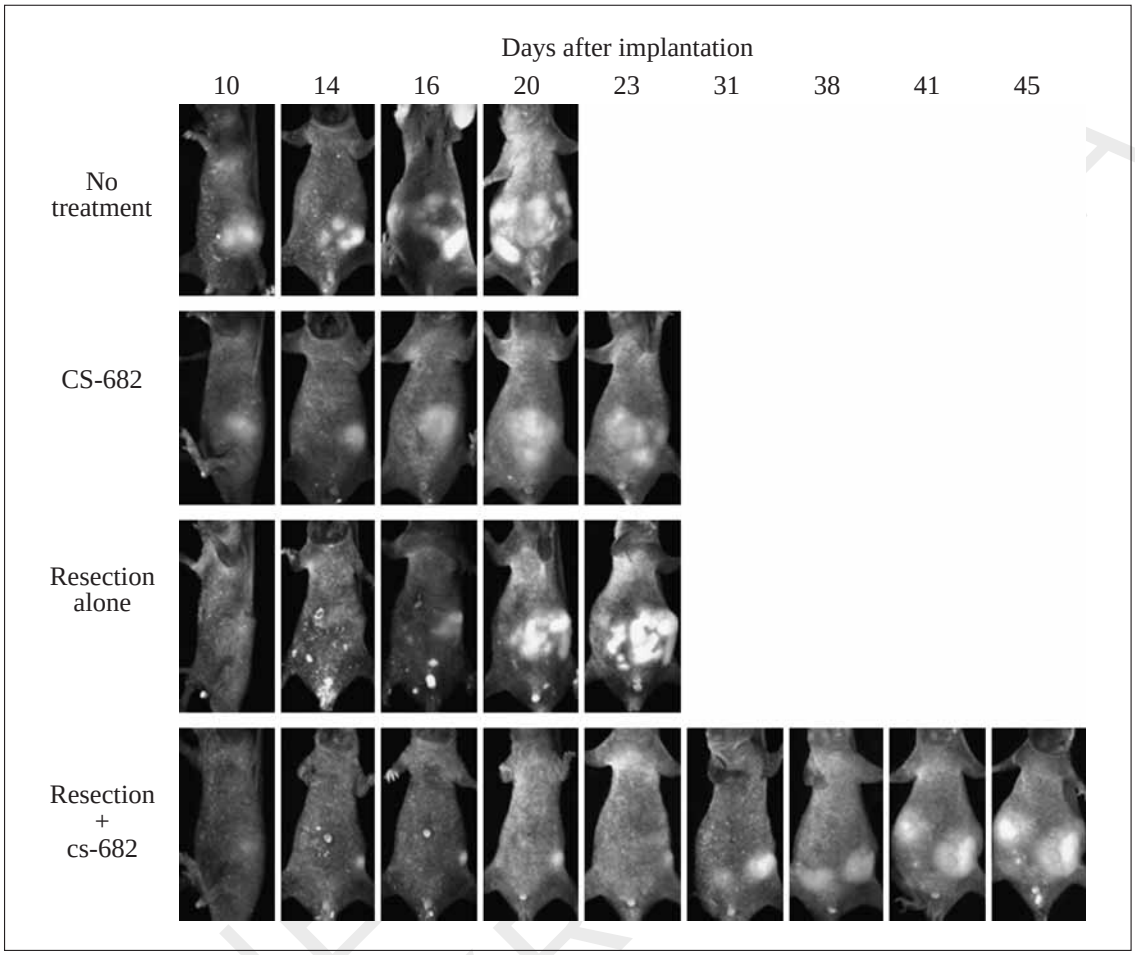

Figure 11.—Sequential, whole body images of one representative mouse from each of four treatment groups. Real time evaluation of therapeutic interventions on pancreatic tumor growth and metastasis was facilitated in this non-invasive system using fluorescence visualization. Resection was performed on day 7 in both the resection and adjuvant groups; CS-682 was initiated in the primary and adjuvant groups at a dose of 50 mg/kg on day 9. The inhibitory effects of each treatment group on the growth and dissemination of orthotopically implanted human pancreatic tumors were visible in the live mouse by fluorescence imaging.[62]

The genetically-modified strain of *S. typhimurium* requires the amino acids arginine and leucine.[73-75] These mutations preclude growth in normal tissue but do not reduce bacterial virulence in tumor cells. The tumor-targeting strain of S. typhimurium, termed A1-R and expressing GFP, invaded and replicated intracellularly in XPA1 human pancreatic cancer cells expressing GFP in the nucleus and RFP in the cytoplasm. Intracellular bacterial infection led to cell fragmentation and cell death (Figure 12). A1-R was administered to an orthotopic human pancreatic tumor expressing RFP in nude mice. After seven days of treatment, the pancreatic cancer had regressed without the need of chemotherapy or any other treatment. In another study, we demonstrated the efficacy of locally- as well as systemically-administered A1-R on liver metastasis of pancreatic cancer.[76] Mice treated with A1-R given locally via intrasplenic injections or systemically via tail vein injections had a much lower hepatic and splenic tumor burden compared with control mice. Systemic treatment with intravenous A1-R also increased sur-

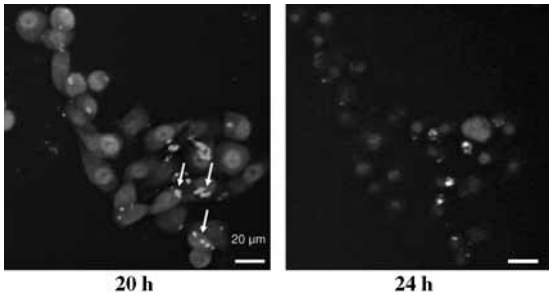

Figure 12.—Intracellular growth of S. typhimurium A1-R in vitro. XPA1 cells labeled with RFP in the cytoplasm and GFP in the nucleus.[72] Interaction between bacteria and tumor cells was observed at the indicated time points under fluorescence microscopy. A, B) GFP expressing S. typhimurium A1-R (arrows) was able to invade and replicate intracellularly in the dual-color XPA1 cell line in vitro. The cytopathic effects of A1-R on XPA1 cells after infection were visible using dual-color fluorescence. Intracellular bacterial infection leading to eventual cell fragmentation and cell death was observed (B). Bars: 20 μm.

vival time. All results were statistically significant. This new strategy demonstrates the clinical potential of bacterial targeting for pancreatic cancer.

Color-coded imaging of pancreatic cancer angiogenesis

Dual-color imaging of nascent blood vessels vascularizing pancreatic cancer in an orthotopic model demonstrated anti-angiogenesis efficacy of gemcitabine.[63] The stem cell marker nestin has recently been shown to be expressed in the pancreas (Figure 13) and in nascent blood vessels in nestin-driven green fluorescent protein (ND-GFP) transgenic nude mice. We visualized by dual-color fluorescence

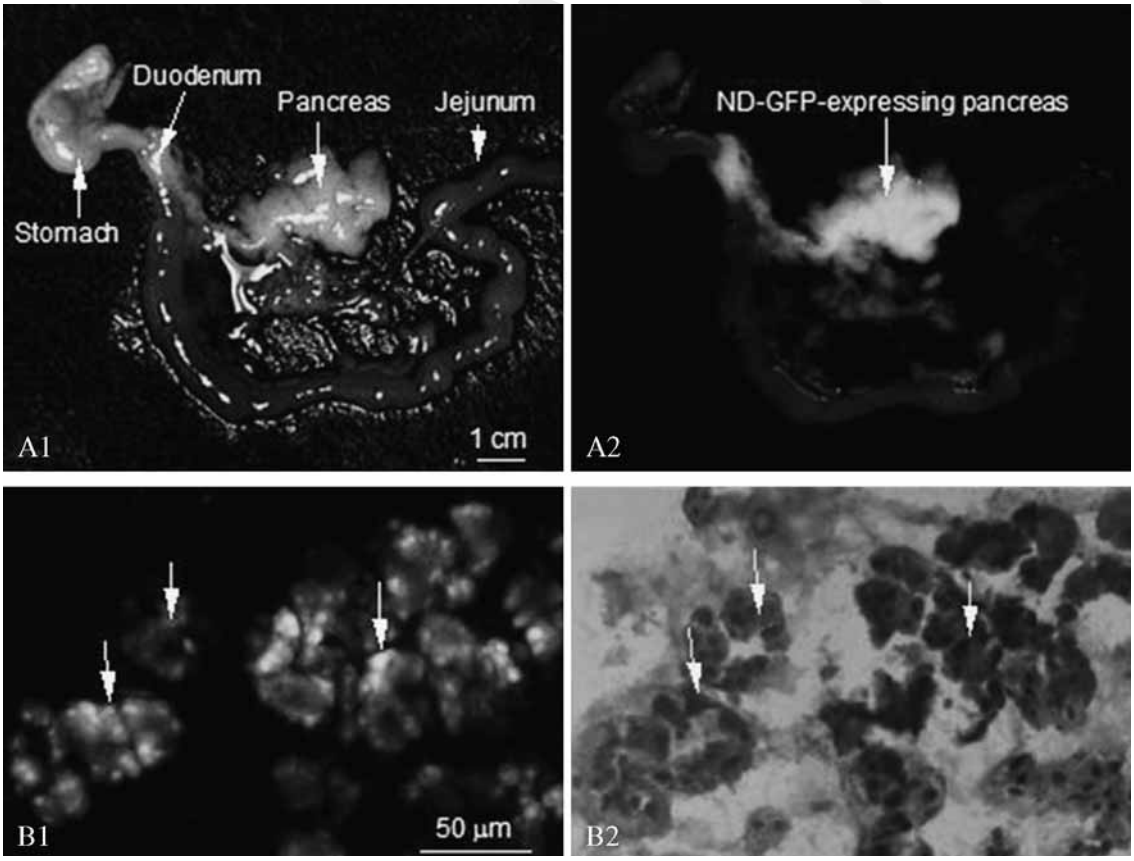

Figure 13.—ND-GFP expression in the pancreas. The pancreas in ND-GFP transgenic nude mice, (A1) bright field; (A2) fluorescence. Acinar cells of the pancreas in the ND-GFP transgenic nude mice (arrows), (B1) fluorescence; (B2) bright field.[63]

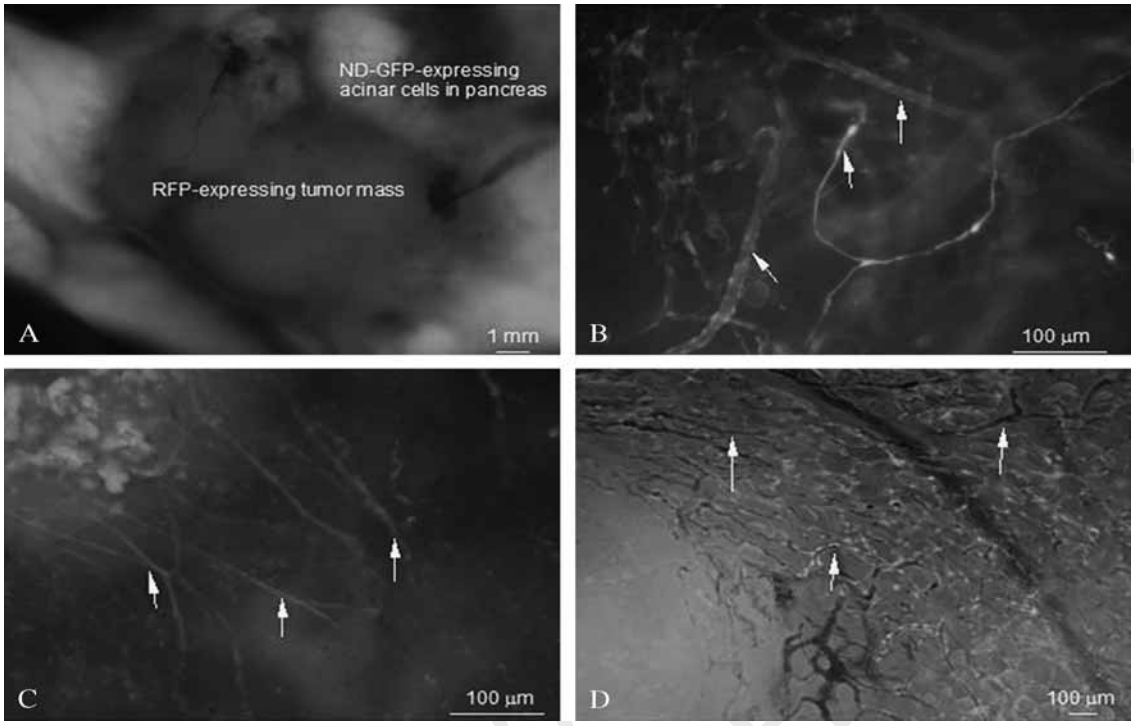

Figure 14.—Dual-color imaging of nascent blood vessels in the orthotopically growing MIAPaCa-2 pancreatic tumor. A-D) Day-14 after orthotopic implantation of RFP-expressing MIAPaCa-2 human pancreatic cancer cells to ND-GFP transgenic nude mice; A) The RFP-expressing MIAPaCa-2 human pancreas tumor growing in the ND-GFP expressing pancreas in an ND-GFP transgenic nude mouse; B-D) The ND-GFP-expressing nascent blood vessels (white arrows) growing in the RFP-expressing tumor mass; D) newly formed ND-GFP-expressing blood vessels with blood flow.[63]

imaging tumor angiogenesis in the ND-GFP transgenic nude mice after orthotopic transplantation of the MIA PaCa-2 human pancreatic cancer line expressing RFP. Mice were treated with gemcitabine at 150 mg/kg/dose on days 3, 6, 10, and 13 after tumor implantation. At day 14, mice were sacrificed and mean nascent blood vessel density and tumor volume were calculated and compared to control mice. ND-GFP was highly expressed in proliferating endothelial cells and nascent blood vessels in the growing tumor (Figures 13, 14). Results of immunohistochemical staining showed that the endothelial marker CD31 co-localized in ND-GFP-expressing nascent blood vessels. The density of nascent blood vessels in the tumor was readily quantified by GFP imaging. Gemcitabine significantly decreased the mean nascent blood vessel density in the tumor as well as decreased tumor volume. The dual-color model of the ND-GFP nude mouse orthotopically implanted with RFP-expressing pancreatic tumor cells enabled the simultaneous visualization and quantification of tumor angiogenesis and tumor volume. These results demonstrated for the first time that gemcitabine is an inhibitor of angiogenesis as well as tumor growth in pancreatic cancer. The results have important implications for the clinical application of gemcitabine in this disease.

Dual-color imaging of nascent blood vessels vascularizing liver metastasis of pancreatic cancer also demonstrated antiangiogenesis efficacy of gemcitabine.[64] We have developed a model of angiogenesis of pancreatic cancer liver metastases in the nude mouse as outlined in Figure 15. Nascent angiogenesis of pancreatic cancer liver metastasis in the ND-GFP transgenic nude mice, which formed after splenic injection of low-passage xPA-1 human pancreatic cancer cells expressing RFPl, was visualized by dual-color fluorescence imaging. ND-GFP was highly expressed in proliferating endothelial cells

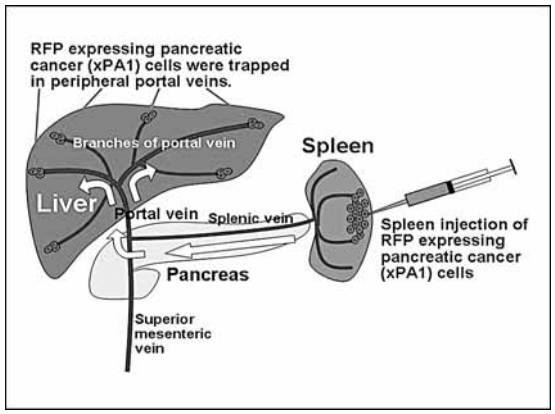

Figure 15.—Experimental model of liver metastases of pancreatic cancer. ND-GFP transgenic nude mice, 6-8 weeks old, were used. The mice were anesthetized with tribromoethanol. xPA1-RFP cells, grown in RPMI medium with 10% fetal bovine serum, were detached from the culture flask by a brief incubation with phosphate-buffered saline without calcium and magnesium containing 2 mM EDTA. The cancer cells were suspended in RPMI 1 640/10% FBS, washed and resuspended in PBS. Fifty microliters containing 2x106 xPA1-RFP cells per mouse were injected in the spleen with a 27G syringe.[64]

and nascent blood vessels in the growing liver metastasis. Immunohistochemical staining showed that CD31 co-localized in ND-GFP-expressing nascent blood vessels. The density of nascent blood vessels in the tumor was readily quantified. Gemcitabine significantly decreased the mean nascent blood vessel density in the pancreatic liver metastases (Figure 16). Thus, the dual-color model of the ND-GFP nude mouse, with RFP-expressing pancreatic cancer liver metastases, enabled the visualization and quantitation of nascent angiogenesis in the metastasis and its response to the angiogenic inhibitory activity of gemcitabine.

The cyan fluorescent protein (CFP) transgenic mouse as a model for imaging pancreatic exocrine cells

By using whole-body and organ-specific fluorescence imaging, we characterized the transgenic cyan fluorescent protein (CFP) mouse.[77] Mice were imaged using two devices. Brightfield images were obtained with the OV100 Small Animal Imaging System (Olympus Corp., Tokyo, Japan). Fluorescence imaging was performed under the CFP filter using the iBox Small Animal Imaging System (UVP, Upland, CA, USA). All animals were sacrificed immediately before imaging. They were imaged before and throughout multiple steps of a complete necropsy. Harvested organs were also imaged with both devices. Selected organs were then frozen and processed for histology, fluorescence microscopy, and H&E staining. Fluorescence microscopy was performed with an Olympus IMT-2 inverted fluorescence microscope. Surprisingly, we found that there is differential enhancement of fluorescence among organs; most notably, the pancreas stands out from the rest of the gastrointestinal tract, displaying the strongest fluorescence of all organs in the CFP mouse.[78] Fluorescence

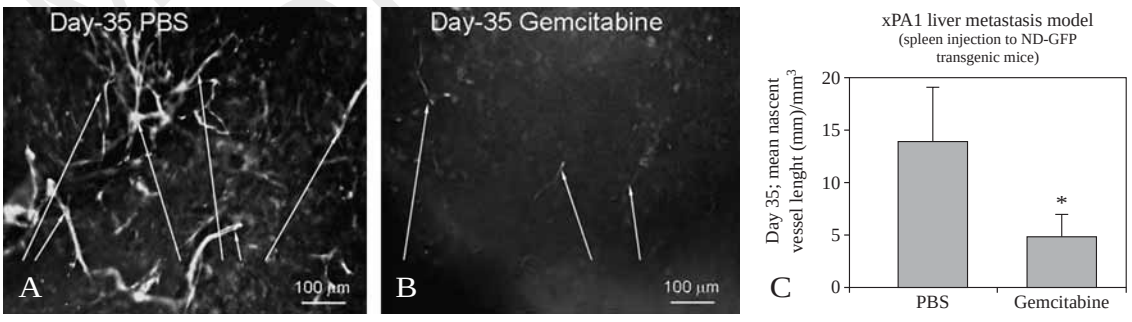

Figure 16.—Anti-angiogenic effect of gemcitabine on xPA-1-RFP pancreatic liver metastases. A) Control mice were given ip injections of PBS. In the control mice, the ND-GFP-expressing nascent blood vessels formed a network in the growing tumor mass; B) mice were given ip injections of gemcitabine. In the treated mice, the ND-GFP-expressing nascent blood vessels were diminished; C) by day-35 after splenic injection, the mean nascent blood vessel density in the gemcitabine-treated mice was significantly less than the PBS-injected mice ($P<0.05$).[64]

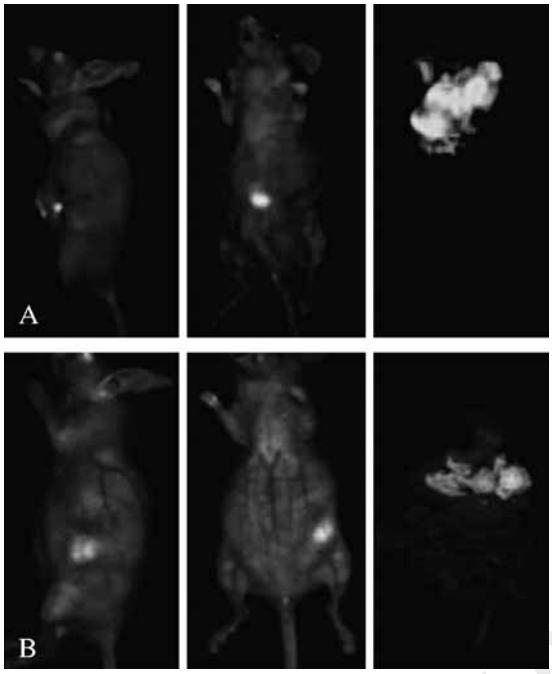

Figure 17.—Imaging the orthotopic human pancreatic cancer CFP nude mouse model with XPA-1-RFP cells.[79] Orthotopic injection of human pancreatic cancer cells was performed in CFP nude mice. These images were obtained at week 6 post-implantation. Exposure time for CFP signals was 1 s. A: In this series, whole-body dual-color imaging permits identification of the tumor in the animal. This brightly red fluorescent tumor had grown extensively into the blue pancreas. This could be seen after isolation of the GI tract, where only small slivers of blue pancreas could be seen around the red tumor. B: The dual-colored XPA-1-GFP-RFP tumor was grown from human pancreatic cancer cells engineered to express orthotopic GFP in the nucleus and RFP in the cytoplasm. Whole body tri-color intact imaging permitted identification of the tumor within the mouse. After isolation of the GI tract, one could see a dual-colored tumor sitting on a blue-fluorescent pancreas.

micro-scopy demonstrated that the CFP fluorescence resided in the acinar cells of the pancreas and not the islet cells. The CFP mouse should lead to a deeper understanding of pancreatic function and pathology, including cancer.

Development of CFP-expressing nude mouse for "Technicolor" cancer imaging

A major goal for *in vivo* biology is to develop models which can express multiple colors of fluorescent proteins in order to image many processes simultaneously in real time. Towards this goal, the CFP nude mouse was developed by crossing non-transgenic nude mice with the transgenic CK/ECFP mouse in which the beta-actin promoter drives expression of CFP in almost all tissues.[77] In crosses between nu/nu CFP male mice and nu/+ CFP female mice, approximately 50% of the embryos fluoresced blue.[79] In the CFP nude mice, the pancreas and reproductive organs displayed the strongest fluorescent signals of all internal organs which vary in intensity. Orthotopic implantation of XPA-1 human pancreatic cancer cells expressing RFP, or expressing GFP in the nucleus and RFP in the cytoplasm, was performed in female nude CFP mice (Figure 17). Color-coded fluorescence imaging of these human pancreatic cancer cells implanted into the bright blue fluorescent pancreas of the CFP nude mouse afforded novel insight into the interaction of the pancreatic tumor and the normal pancreas, in particular the strong desmoplastic reaction of the tumor (Figure 18). The naturally enhanced blue fluorescence of the pancreas in the CFP mouse serves as an ideal background for color-coded imaging of the interaction of implanted cancer cells and the host. The CFP nude mouse will provide unique understanding of the critical interplay between the cancer cells and their microenvironment.

Conclusions

Here we describe our cumulative experience with the development and preclinical application of several fluorescent, clinically-relevant, orthotopic metastatic mouse models of pancreatic cancer. These models utilize the human pancreatic cancer cell lines which have been genetically engineered to selectively express high levels of GFP or RFP. Locoregional tumor growth and distant metastasis of these orthotopic implants occurs spontaneously and rapidly throughout the abdomen in a manner consistent with clinical human disease. Highly specific, high-resolution, real-time visualization of tumor growth and metastasis was achieved *in vivo* without the need for contrast agents, inva-

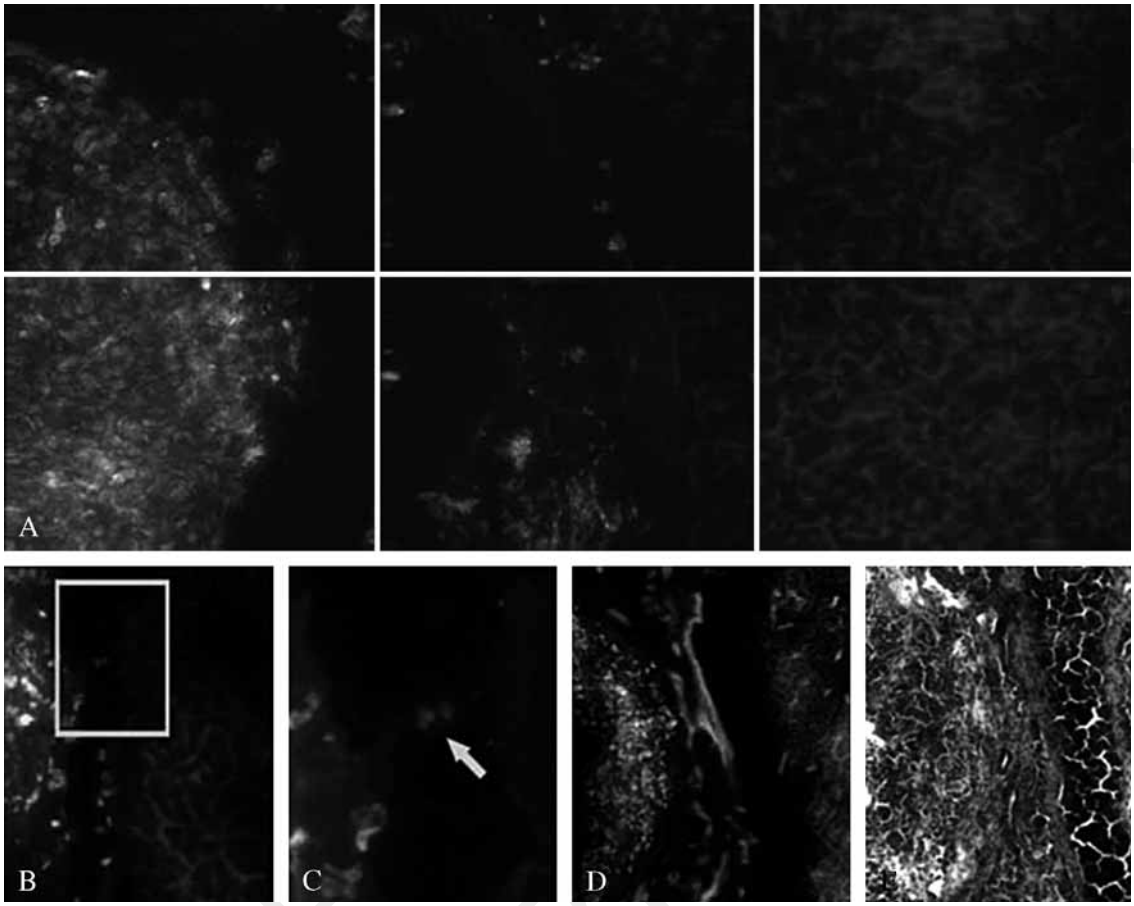

Figure 18.—Color-coded fluorescence microscopy of the pancreatic tumor microenvironment in the CFP nude mouse.[79] The dual-colored pancreatic tumor was removed en bloc and frozen in OTC, and subsequently imaged under fluorescence microscopy. A) A high-resolution deconvolved image of the tumor-host interaction area is shown. The blue fluorescent pancreas in invaded by the dual-colored XPA-1-GFP-RFP cells, with an intervening area of dense fibrous tissue infiltrated by only few tumor cells; B,C) A dividing tumor cell (arrow) is identified at the edge of this interaction zone, near the pancreas; D) CD31 staining for blood vessels confirms the increased vascularity of this interaction zone; E) H&E staining of this area is attached for comparison.

sive techniques, or expensive imaging equipment. Transplantation of tumor fragments onto the pancreas of GFP- or CFP-expressing transgenic mice may be used to facilitate visualization of tumor-host interaction between the pancreatic tumor and host-derived stroma and vasculature. Such *in vivo* models have enabled us to serially visualize and acquire images of the progression of pancreatic cancer in the live animal, and to demonstrate the real-time antitumor, antimetastatic, and antiangiogenesis efficacy of several novel therapeutic strategies on pancreatic malignancy. These fluorescent models are therefore powerful and reliable tools with which to investigate human pancreatic cancer and novel therapeutic strategies directed against it.

Riassunto

Modelli ortotopici metastatici di cancro pancreatico clinicamente rilevanti visualizzabili tramite reporter genetici fluorescenti

Questo articolo descrive l'esperienza accumulata dagli autori con lo sviluppo e l'applicazione pre-clinica di modelli ortotopici metastatici di cancro pancreatico clinicamente rilevanti visualizzabili tramite reporter

genetici fluorescenti. Questi modelli utilizzano cellule di cancro pancreatico umano, in precedenza geneticamente modificate per esprimere selettivamente elevati livelli della proteina fluorescente verde (*green fluorescent protein*, GFP) o della proteina fluorescente rossa (*red fluorescent protein*, RFP). I tumori con reporter genetici fluorescenti vengono impiantati nel tessuto sottocutaneo in topi nudi, quindi dei frammenti di tumori sottocutanei vengono chirurgicamente impiantati sul pancreas. La crescita tumorale loco-regionale e le metastasi a distanza di questi impianti ortotopici avvengono spontaneamente e rapidamente all'interno dell'addome con modalità molto simile a quella della malattia nell'uomo. L'imaging di fluorescenza quantitativa altamente specifico, ad elevata risoluzione, in tempo reale della crescita tumorale e delle metastasi può essere ottenuto *in vivo* senza la necessità di utilizzare mezzi di contrasto, tecniche invasive, o metodiche di imaging costose. Gli autori hanno dimostrato un'elevata correlazione tra l'imaging ottico a fluorescenza, l'imaging della risonanza magnetica, e l'ecografia in questi modelli animali. Il trapianto di frammenti di tumore che esprimono RFP sul pancreas di topi transgenici che esprimono GFP o la proteina ciano fluorescente è stato utilizzato per facilitare la visualizzazione dell'interazione tumore-ospite tra le cellule del carcinoma pancreatico e lo stroma e la vascolarizzazione ottenuti dall'ospite. Tali modelli *in vivo* hanno consentito agli autori di visualizzare in tempo reale e acquisire immagini della progressione del carcinoma pancreatico nell'animale in vita, e di dimostrare gli effetti anti-tumorali e anti-metastatici sempre in tempo reale di diverse nuove strategie terapeutiche nei confronti del carcinoma pancreatico. Questi modelli fluorescenti sono pertanto strumenti validi e affidabili con cui studiare il carcinoma pancreatico metastatico dell'uomo e nuove strategie terapeutiche dirette contro questa neoplasia.

Parole chiave: Proteina fluorescente verde - Proteina fluorescente rossa - Proteina fluorescente cyan - Pancreas - Neoplasia del pancreas - Modelli animali.

References

1. Bouvet M, Gamagami RA, Gilpin EA, Romeo O, Sasson A, Easter DW *et al.* Factors influencing survival after resection for periampullary neoplasms. Am J Surg 2000;180:13-7.
2. Katz MH, Bouvet M, Al-Refaie W, Gilpin EA, Moossa AR. Non-pancreatic periampullary adenocarcinomas: an explanation for favorable prognosis. Hepatogastroenterology 2004;51:842-6.
3. Bouvet M, Binmoeller KF, Moossa AR. Diagnosis of adenocarcinoma of the pancreas. In: Cameron JL, editor. American Cancer Society Atlas of Clinical Oncology: pancreatic cancer. Hamilton, ON: BC Decker; 2001.
4. Moossa AR, Bouvet M, Gamagami R. The pancreas. In: Cuschieri A, Steele RJC, Moossa AR, editors. Essential surgical practice. 4th ed. London: Arnold Publishing; 2002. p. 477-525.
5. Katz MH, Savides TJ, Moossa AR, Bouvet M. An evidence-based approach to the diagnosis and staging of pancreatic cancer. Pancreatology 2005;5:576-90.
6. Bouvet M, Yang M, Nardin S, Wang X, Jiang P, Baranov E *et al.* Chronologically-specific metastatic targeting of human pancreatic tumors in orthotopic models. Clin Exp Metastasis 2000;18:213-8.
7. Bouvet M, Wang J, Nardin SR, Nassirpour R, Yang M, Baranov E *et al.* Real-time optical imaging of primary tumor growth and multiple metastatic events in a pancreatic cancer orthotopic model. Cancer Res 2002;62:1534-40.
8. Marincola FM, Drucker BJ, Siao DY, Hough KL, Holder WD Jr. The nude mouse as a model for the study of human pancreatic cancer. J Surg Res 1989;47:520-9.
9. Bruns CJ, Harbison MT, Kuniyasu H, Eue I, Fidler IJ. *In vivo* selection and characterization of metastatic variants from human pancreatic adenocarcinoma by using orthotopic implantation in nude mice. Neoplasia 1999; 1:50-62.
10. Vezeridis MP, Doremus CM, Tibbetts LM, Tzanakakis G, Jackson BT. Invasion and metastasis following orthotopic transplantation of human pancreatic cancer in the nude mouse. J Surg Oncol 1989;40:261-5.
11. Fu X, Guadagni F, Hoffman RM. A metastatic nude-mouse model of human pancreatic cancer constructed orthotopically with histologically intact patient specimens. Proc Natl Acad Sci U S A 1992;89:5645-9.
12. An Z, Wang X, Kubota T, Moossa AR, Hoffman RM. A clinical nude mouse metastatic model for highly malignant human pancreatic cancer. Anticancer Res 1996;16:627-31.
13. Furukawa T, Kubota T, Watanabe M, Kitajima M, Hoffman RM. A novel patient-like treatment model of human pancreatic cancer constructed using orthotopic transplantation of histologically intact human tumor tissue in nude mice. Cancer Res 1993;53:3070-2.
14. Kiguchi K, Kubota T, Aoki D, Udagawa Y, Yamanouchi S, Saga M *et al.* A patient-like orthotopic implantation nude mouse model of highly metastatic human ovarian cancer. Clin Exp Metastasis 1998;16:751-6.
15. Tomikawa M, Kubota T, Matsuzaki SW, Takahasi S, Kitajima M, Moossa AR *et al.* Mitomycin C and cisplatin increase survival in a human pancreatic cancer metastatic model. Anticancer Res 1997;17:3623-5.
16. Kyriazis AP, DiPersio L, Michael GJ, Pesce AJ, Stinnett JD. Growth patterns and metastatic behavior of human tumors growing in athymic mice. Cancer Res 1978;38:3186-90.
17. Fidler IJ. Critical factors in the biology of human cancer metastasis: twenty-eighth G.H.A. Clowes memorial award lecture. Cancer Res 1990;50:6130-8.
18. Fidler IJ. Rationale and methods for the use of nude mice to study the biology and therapy of human cancer metastasis. Cancer Metastasis Rev 1986;5:29-49.
19. Miller FR, Medina D, Heppner GH. Preferential growth of mammary tumors in intact mammary fatpads. Cancer Res 1981;41:3863-7.
20. Sordat B, Wang WR. Human colorectal tumor xenografts in nude mice: expression of malignancy. Behring Inst Mitt 1984;(74):291-300.
21. Morikawa K, Walker SM, Nakajima M, Pathak S, Jessup JM, Fidler IJ. Influence of organ environment on the growth, selection, and metastasis of human colon carcinoma cells in nude mice. Cancer Res 1988;48: 6863-71.
22. Hoffman RM. Orthotopic metastatic mouse models for anticancer drug discovery and evaluation: a bridge to the clinic. Invest New Drugs 1999;17:343-59.
23. Tan MH, Chu TM. Characterization of the tumorigenic and metastatic properties of a human pancreatic tumor

cell line (AsPC-1) implanted orthotopically into nude mice. Tumour Biol 1985;6:89-98.
24. US Patents 5, 284 and 5,569,812 Reissue RE:39,337.
25. Lin WC, Pretlow TP, Pretlow TG 2nd, Culp LA. Bacterial lacZ gene as a highly sensitive marker to detect micrometastasis formation during tumor progression. Cancer Res 1990;50:2808-17.
26. Fukumura D, Yuan F, Monsky WL, Chen Y, Jain RK. Effect of host microenvironment on the microcirculation of human colon adenocarcinoma. Am J Pathol 1997;151:679-88.
27. Chambers AF, MacDonald IC, Schmidt EE, Koop S, Morris VL, Khokha R *et al.* Steps in tumor metastasis: new concepts from intravital videomicroscopy. Cancer Metastasis Rev 1995;14:279-301.
28. Weissleder R, Tung CH, Mahmood U, Bogdanov A Jr. *In vivo* imaging of tumors with protease-activated near-infrared fluorescent probes. Nat Biotechnol 1999;17: 375-8.
29. Sweeney TJ, Mailander V, Tucker AA, Olomu AB, Zhang W, Cao Y *et al.* Visualizing the kinetics of tumor-cell clearance in living animals. Proc Natl Acad Sci U S A 1999;96:12044-9.
30. Cheng L, Fu J, Tsukamoto A, Hawley RG. Use of green fluorescent protein variants to monitor gene transfer and expression in mammalian cells. Nat Biotechnol 1996;14:606-9.
31. Chalfie M, Tu Y, Euskirchen G, Ward WW, Prasher DC. Green fluorescent protein as a marker for gene expression. Science 1994;263:802-5.
32. Astoul P, Colt HG, Wang X, Hoffman RM. A "patient-like" nude mouse model of parietal pleural human lung adenocarcinoma. Anticancer Res 1994;14:85-91.
33. Yang F, Moss LG, Phillips GN Jr. The molecular structure of green fluorescent protein. Nat Biotechnol 1996;14:1246-51.
34. Prasher DC, Eckenrode VK, Ward WW, Prendergast FG, Cormier MJ. Primary structure of the Aequorea victoria green-fluorescent protein. Gene 1992;111: 229-33.
35. Zolotukhin S, Potter M, Hauswirth WW, Guy J, Muzyczka N. A "humanized" green fluorescent protein cDNA adapted for high-level expression in mammalian cells. J Virol 1996;70:4646-54.
36. Heim R, Cubitt AB, Tsien RY. Improved green fluorescence. Nature 1995;373:663-4.
37. Delagrave S, Hawtin RE, Silva CM, Yang MM, Youvan DC. Red-shifted excitation mutants of the green fluorescent protein. Biotechnology (N Y) 1995;13:151-4.
38. Cormack BP, Valdivia RH, Falkow S. FACS-optimized mutants of the green fluorescent protein (GFP). Gene 1996;173:33-8.
39. Budinger TF, Benaron DA, Koretsky AP. Imaging transgenic animals. Annu Rev Biomed Eng 1999;1:611-48.
40. Flotte TR, Beck SE, Chesnut K, Potter M, Poirier A, Zolotukhin S. A fluorescence video-endoscopy technique for detection of gene transfer and expression. Gene Ther 1998;5:166-73.
41. Fu XY, Besterman JM, Monosov A, Hoffman RM. Models of human metastatic colon cancer in nude mice orthotopically constructed by using histologically intact patient specimens. Proc Natl Acad Sci U S A 1991;88:9345-9.
42. Sun FX, Sasson AR, Jiang P, An Z, Gamagami R, Li L *et al.* An ultra-metastatic model of human colon cancer in nude mice. Clin Exp Metastasis 1999;17:41-8.
43. Chishima T, Miyagi Y, Wang X, Yamaoka H, Shimada H, Moossa AR *et al.* Cancer invasion and micrometastasis visualized in live tissue by green fluorescent protein expression. Cancer Res 1997;57:2042-7.
44. Chishima T, Miyagi Y, Wang X, Baranov E, Tan Y, Shimada H *et al.* Metastatic patterns of lung cancer visualized live and in process by green fluorescence protein expression. Clin Exp Metastasis 1997;15:547-52.
45. Chishima T, Miyagi Y, Wang X, Tan Y, Shimada H, Moossa A *et al.* Visualization of the metastatic process by green fluorescent protein expression. Anticancer Res 1997;17:2377-84.
46. Chishima T, Miyagi Y, Li L, Tan Y, Baranov E, Yang M *et al.* Use of histoculture and green fluorescent protein to visualize tumor cell host interaction [letter]. In Vitro Cell Dev Biol Anim 1997;33:745-7.
47. Chishima T, Yang M, Miyagi Y, Li L, Tan Y, Baranov E *et al.* Governing step of metastasis visualized in vitro. Proc Natl Acad Sci U S A 1997;94:11573-6.
48. Yang M, Hasegawa S, Jiang P, Wang X, Tan Y, Chishima T *et al*. Widespread skeletal metastatic potential of human lung cancer revealed by green fluorescent protein expression. Cancer Res 1998;58:4217-21.
49. Yang M, Jiang P, Sun FX, Hasegawa S, Baranov E, Chishima T *et al.* A fluorescent orthotopic bone metastasis model of human prostate cancer. Cancer Res 1999;59:781-6.
50. Yang M, Jiang P, An Z, Baranov E, Li L, Hasegawa S *et al.* Genetically fluorescent melanoma bone and organ metastasis models. Clin Cancer Res 1999;5:3549-59.
51. Yang M, Baranov E, Jiang P, Sun FX, Li XM, Li L *et al.* Whole-body optical imaging of green fluorescent protein-expressing tumors and metastases. Proc Natl Acad Sci U S A 2000;97:1206-11.
52. Yang M, Baranov E, Moossa AR, Penman S, Hoffman RM. Visualizing gene expression by whole-body fluorescence imaging. Proc Natl Acad Sci U S A 2000;97:12278-82.
53. Yang M, Baranov E, Li XM, Wang JW, Jiang P, Li L *et al.* Whole-body and intravital optical imaging of angiogenesis in orthotopically implanted tumors. Proc Natl Acad Sci U S A 2001;98:2616-21.
54. Yang M, Baranov E, Wang JW, Jiang P, Wang X, Sun FX *et al.* Direct external imaging of nascent cancer, tumor progression, angiogenesis, and metastasis on internal organs in the fluorescent orthotopic model. Proc Natl Acad Sci U S A 2002;99:3824-9.
55. Hoffman RM. The multiple uses of fluorescent proteins to visualize cancer *in vivo*. Nat Rev Cancer 2005;5:796-806.
56. Katz MH, Takimoto S, Spivack D, Moossa AR, Hoffman RM, Bouvet M. A novel red fluorescent protein orthotopic pancreatic cancer model for the preclinical evaluation of chemotherapeutics. J Surg Res 2003;113:151-60.
57. Katz MH, Spivack DE, Takimoto S, Fang B, Burton DW, Moossa AR *et al.* Gene therapy of pancreatic cancer with green fluorescent protein and tumor necrosis factor-related apoptosis-inducing ligand fusion gene expression driven by a human telomerase reverse transcriptase promoter. Ann Surg Oncol 2003;10:762-72.
58. Katz MH, Takimoto S, Spivack D, Moossa AR, Hoffman RM, Bouvet M. An imageable highly metastatic orthotopic red fluorescent protein model of pancreatic cancer. Clin Exp Metastasis 2004;21:7-12.
59. Tsuji K, Yang M, Jiang P, Maitra A, Kaushal S, Yamauchi K *et al.* Common bile duct injection as a novel method for establishing red fluorescent protein (RFP)-expressing human pancreatic cancer in nude mice. JOP 2006;7:193-9.
60. Bouvet M, Spernyak J, Katz MH, Mazurchuk RV, Takimoto S, Bernacki R *et al.* High correlation of whole-body red fluorescent protein imaging and magnetic resonance imaging on an orthotopic model of pancreatic cancer. Cancer Res 2005;65:9829-33.
61. Katz MH, Bouvet M, Takimoto S, Spivack D, Moossa AR, Hoffman RM. Selective antimetastatic activity of

cytosine analog CS-682 in a red fluorescent protein orthotopic model of pancreatic cancer. Cancer Res 2003;63:5521-5.
62. Katz MH, Bouvet M, Takimoto S, Spivack D, Moossa AR, Hoffman RM. Survival efficacy of adjuvant cytosine-analogue CS-682 in a fluorescent orthotopic model of human pancreatic cancer. Cancer Res 2004;64:1828-33.
63. Amoh Y, Li L, Tsuji K, Moossa AR, Katsuoka K, Hoffman RM *et al.* Dual-color imaging of nascent blood vessels vascularizing pancreatic cancer in an orthotopic model demonstrates antiangiogenesis efficacy of gemcitabine. J Surg Res 2006;132:164-9.
64. Amoh Y, Nagakura C, Maitra A, Moossa AR, Katsuoka K, Hoffman RM *et al.* Dual-color imaging of nascent angiogenesis and its inhibition in liver metastases of pancreatic cancer. Anticancer Res 2006;26:3237-42.
65. Yang M, Li L, Jiang P, Moossa AR, Penman S, Hoffman RM. Dual-color fluorescence imaging distinguishes tumor cells from induced host angiogenic vessels and stromal cells. Proc Natl Acad Sci U S A 2003;100: 14259-62..
66. Saito N, Zhao M, Li L, Baranov E, Yang M, Ohta Y *et al.* High efficiency genetic modification of hair follicles and growing hair shafts. Proc Natl Acad Sci U S A 2002;99:13120-4.
67. Lee NC, Bouvet M, Nardin S, Jiang P, Baranov E, Rashidi B *et al.* Antimetastatic efficacy of adjuvant gemcitabine in a pancreatic cancer orthotopic model. Clin Exp Metastasis 2000;18:379-84.
68. Hoffman RM, Yang M. Whole-body imaging with fluorescent proteins. Nat Protoc 2006;1:1429-38.
69. Yang M, Jiang P, Hoffman RM. Whole-body subcellular multicolor imaging of tumor-host interaction and drug response in real time. Cancer Res 2007;67: 5195-200.
70. Makale M, McElroy M, O'Brien P, Hoffman RM, Guo S, Bouvet M *et al.* Extended-working-distance multiphoton micromanipulation microscope for deep-penetration imaging in live mice and tissue. J Biomed Opt 2009;14:024032.
71. Snyder CS, Kaushal S, Kono Y, Tran Cao HS, Hoffman RM, Bouvet M. Complementarity of ultrasound and fluorescence imaging in an orthotopic mouse model of pancreatic cancer. BMC Cancer 2009;9:106.
72. Nagakura C, Hayashi K, Zhao M, Yamauchi K, Yamamoto N, Tsuchiya H *et al.* Efficacy of a Genetically-modified Salmonella typhimurium in an Orthotopic Human Pancreatic Cancer in Nude Mice. Anticancer Res 2009;29:1873-8.
73. Zhao M, Geller J, Ma H, Yang M, Penman S, Hoffman RM. Monotherapy with a tumor-targeting mutant of Salmonella typhimurium cures orthotopic metastatic mouse models of human prostate cancer. Proc Natl Acad Sci U S A 2007;104:10170-4.
74. Zhao M, Yang M, Li XM, Jiang P, Baranov E, Li S *et al.* Tumor-targeting bacterial therapy with amino acid auxotrophs of GFP-expressing Salmonella typhimurium. Proc Natl Acad Sci U S A 2005;102:755-60.
75. Zhao M, Yang M, Ma H, Li X, Tan X, Li S *et al.* Targeted therapy with a Salmonella typhimurium leucine-arginine auxotroph cures orthotopic human breast tumors in nude mice. Cancer Res 2006;66:7647-52.
76. Yam C, Zhao M, Hayashi K, Ma H, Kishimoto H, McElroy M *et al.* Monotherapy with a tumor-targeting mutant of S. typhimurium inhibits liver metastasis in a mouse model of pancreatic cancer. J Surg Res 2009 [In press].
77. Hadjantonakis AK, Macmaster S, Nagy A. Embryonic stem cells and mice expressing different GFP variants for multiple non-invasive reporter usage within a single animal. BMC Biotechnol 2002;2:11.
78. Tran Cao HS, Kimura H, Kaushal S, Snyder CS, Reynoso J, Hoffman RM *et al.* The cyan fluorescent protein (CFP) transgenic mouse as a model for imaging pancreatic exocrine cells. JOP 2009;10:152-6.
79. Tran Cao HS, Reynoso J, Yang M, Kimura H, Kaushal S, Snyder CS *et al.* Development of the transgenic cyan fluorescent protein (CFP)-expressing nude mouse for "Technicolor" cancer imaging. J Cell Biochem 2009; 107:328-34.